IEEE Access
Multidisciplinary | Rapid Review | Open Access Journal

Received February 3, 2021, accepted February 19, 2021, date of publication February 24, 2021, date of current version March 4, 2021.

Digital Object Identifier 10.1109/ACCESS.2021.3061657

Prediction of Process Parameters of Ultrasonically Welded PC/ABS Material Using Soft-Computing Techniques

T. CHINNADURAI[1], NATARAJAN PRABAHARAN[2], (Member, IEEE), S. SARAVANAN[3], M. KARTHIGAI PANDEAN[1], P. PANDIYAN[4], AND HASSAN HAES ALHELOU[5], (Senior Member, IEEE)

[1]Department of ICE, Sri Krishna College of Technology, Coimbatore 641008, India
[2]Department of EEE, SASTRA Deemed University, Thanjavur 613401, India
[3]Department of EEE, Sri Krishna College of Technology, Coimbatore 641008, India
[4]Department of EEE, KPR Institute of Engineering, Coimbatore 641402, India
[5]Department of Electrical Power Engineering, Faculty of Mechanical and Electrical Engineering, Tishreen University, Lattakia 2230, Syria

Corresponding author: Hassan Haes Alhelou (alhelou@ieee.org)

ABSTRACT Welding process is found to be a predominant procedure in most of the processing industries, especially in the automobile sector for maintenance operation and fabrication. Ultrasonic Polymer Welding (USW) is used for the joining process because of its flexibility and short needed welding time. In this article, two different polymer materials PC and ABS are blended in the ratio of 60:40 and molded into a sheet. Furthermore, molded PC/ABS sheets are joined using USW with different processing parameter settings. Three major influencing process parameters like pressure (P), amplitude (A) and weld time (Tw) are considered and other processing parameters are kept at constant. The experiment is carried out for 26 welded samples and from the obtained results it is noticed that the above-mentioned process parameters directly influence the tensile strength of welded joints. Additionally, the ultrasonically welded samples tensile strength is analyzed with the help of Artificial Neural Network technique (ANN) and Adaptive Neuro-Fuzzy Inference System method (ANFIS). From the simulation results, an optimized ANFIS model provides the superior result as compared to ANN. Moreover, Scanning Electron Microscope analysis is carried out to visualize the weld interface between the joint. Also, Finite Element Modeling (ANSYS) is performed to understand the heat dissipation during the welding process.

INDEX TERMS ANN, ANFIS, process parameters, tensile strength, ultrasonic welding.

I. INTRODUCTION

Polymers are widely used in several industries like packaging, automotive, and aerospace, among others. In addition, the polymer usage in industry has been improved by blending a pair of individual polymer materials together to create a new blend polymer with the adequate strength for the particular applications. This blended polymer plays a significant contribution in both interior dashboards and wheel cover parts of vehicles [1].

Polycarbonate (PC) and Acrylonitrile–Butadiene–Styrene (ABS) polymers were mixed for analyzing the strength of the material. PC is a flexible thermoplastic material whereas ABS provides good impact resistance, heat resistance and toughness to the thermoplastic polymer [2]. Most of the engineering applications are required to meet heavy loads by having features of high strength along with adaptable nature material.

The main characteristics of ABS material is to reduce the ductile nature of PC as it gets blended, thereby adapting to the intermediate properties of PC and ABS [3] in the resultant blended material. The blended PC/ABS polymer has reached significant attention in engineering applications due to its higher grade of toughness properties as required by the automotive industry. Polymers used in automobile sector undergo various stages to reach their final shape. Besides, joining of two individual parts and selection of joining method will also play a major role in the automotive sector. Among different available joining methods, USW joining method is highly preferred. USW joining is one of the most efficient methods

The associate editor coordinating the review of this manuscript and approving it for publication was Barbara Masini.

for joining polymer and its composites [4]. The blended PC/ABS polymers have been welded by imposing high frequency (20 kHz to 70 kHz) [5] vibrations under different ranges of holding pressure.

The vibrations have been created perpendicular to the portions to be welded by utilizing a high-frequency signal. It produces localized heating to join the materials [6]. The strength of weld produced by the USW method is essentially based on material properties and parameters considered for welding. The key parameters for the welding process are holding time, holding pressure, welding time, welding pressure, amplitude, etc. Among these parameters, pressure, weld time and amplitude have the greatest influence on the weld strength [7]. In addition, the Energy Director (ED) design including size and shape also contributes towards the strength of the welding [8], [9].

It is very tedious processes to determine the optimal parameter since the USW process comprises of more process parameters. All are interrelated between them which leads to an increase in the complexity of parameter setting while welding the material. The above-said complexity of the existing mathematical models failed to elucidate the nonlinear behavior in the USW technique. Hence the involvement of different soft computing techniques such as ANNs and ANFIS is required to overcome the drawback.

ANNs provide a high degree of accuracy in process parameter modeling, and high speed and stability as compared to other traditional methods [10]. Thus, some of ANNs such as Back-Propagation Neural Network (BPNN) and Radial Basis Functions (RBFs) have been employed in modeling and weld quality prediction [11]. Back-propagation algorithm is mainly utilized to train the ANN model in order to categorize the frequency patterns and feedback forces in the friction stir welding process, which is then used for the detection of defects in wormholes [10]. Furthermore, the tensile strength of aluminum alloy used in the FSW procedure has been estimated by developing an ANN model. From the existing study, researchers mostly used ANN models to show a relationship between input and output in various welding procedures [12].

ANFIS modeling integrates two optimization techniques namely ANN and fuzzy systems. ANFIS system is a well suitable tool for dealing with non-linear based systems. A neural network has been employed to correlate the uncertainty condition from the system and output has been determined using exact fuzzy rules available in the fuzzy system. Due to the combined operation of neural network and fuzzy logic control, the controller based an ANFIS gives very accurate outcome in decision-making and control of the system [13]–[15].

The primary motivation of this work is to investigate the weld strength for PC/ABS blend using Artificial Intelligence (AI) techniques. In this work, two different AI techniques namely ANN-BP and ANFIS are proposed to predict better strength from various trials. More detailed analysis is conducted to discover the nature and effect of the input process parameters over the weld strength. The USW process is carried out on blended PC/ABS material and its experimental results are measured. Further, simulation results are compared with obtained experimental results. The correlation between input and output parameters is obtained from a linear model of ANN to improve the performance of the welding process. Likewise, the ANFIS model has been developed to predict the influence of input parameters on weld strength of the PC/ABS joint and finally, the microstructural images have been obtained to analyze the nature of the weld. Finite element analysis (ANSYS) is carried out to examine the deformation pattern with temperature loading. It is worth to mention that the available research literatures based on the FEM modeling is minimum. Therefore, this article utilizes the proposed FEA model to reveal the approximate forecasting of a PC/ABS blend material behavior post-welding.

The main contribution of this work as follows:

- Blending and welding of two dissimilar polymers of PC/ABS in the ratio of 60:40 which provides the high strength to weight ratio.
- Selection of most influencing parameters during the welding using ANN and ANFIS.
- The weld quality and nature of welding portions are analyzed by using SEM images.
- Validating the welded samples with FEM modeling for finding the heat distribution and melting of energy director.

The remaining section of this article as follows: Section II deals with material selection, energy director selection, injection molding, ANN and ANFIS for experimental work, section III discussed the results and discussion and finally the conclusion is discussed in section IV.

II. EXPERIMENTATION

A. MATERIAL SELECTION

The selection of process parameters is important to achieve proper welding. The most influencing parameters are pressure, weld time, EDs design, hold time and amplitude. The selected materials for this work are PC/ABS. The materials are blended using an injection molding machine.

PC is an amorphous plastic material, which is widely used in many engineering applications due to its high impact resistance, transparency nature, high melting temperature and low scratch resistance [16]. It is synthesized from hydrocarbon fuels comprising of fewer weight groups termed as ''fractions''. This fraction catalysis produces PC. The common properties of PC are listed in Table 1. It is observed that the PC has a deficient true melting point distinct from crystalline polymers. However, PC exhibits a property of elevated glass shift in temperature around 150°C [17]. This property makes more complexity in the processing of PC to large melting viscosity, which restricts the fluidity of PC and induces residual stress-producing fractures. Accordingly, the polymer blends are produced to overcome the fracture.

ABS is a combination of Styrene (S), Acrylonitrile (A), and Butadiene (B) polymer. This combination provides improved hardness, heat resistance and rigidity. The properties

TABLE 1. PC material properties.

Properties	Parameters	Values
Mechanical	Compressive Strength (psi)	12,000
	Tensile Strength (psi)	9,500
	Flexural Strength (psi)	15,000
Thermal	Glass Transition Temperature (°C)	145
	Thermal Conductivity (W/(m*K))	0.20
	Heat Deflection Temperature (°C)	140
	Max Operating Temperature (°C)	135
Physical	Density (g/cm³)	1.2

of ABS are listed in Table 2. Based on the composition of ABS, different grades are available to meet the customer's requirements. It is very simple to control three monomers by introducing fibers into the material for enhancing the stiffness of ABS.

TABLE 2. ABS material properties.

Properties	Parameters	Values
Mechanical	Tensile Strength (psi)	7750
	Compressive Strength (psi)	-
	Flexural Strength (psi)	11,800
Physical	Density (g/cm³)	1.05
Thermal	Thermal Conductivity (W/(m*K))	0.25
	Heat Deflection Temperature (°C)	88
	Max Operating Temperature (°C)	105
	Glass Transition Temperature (°C)	105

ABS polymer material is short in desired features, particularly in terms of mechanical property, thereby limiting its employability for several infrastructural applications. To improve its usability, the PC material was blended with ABS materials to form new improved properties [18], [19]. The contribution of Acrylonitrile (A) supplements could increase its heat resistance, chemical resistance and surface hardness whereas the Styrene (S) enhances its strength, rigidity and process-ability. Similarly, Butadiene (B) helps to improve toughness and impact resistance [17]. Finally, the PC/ABS blended polymer gives high tensile strength, heat resistance, and reduced melting viscosity. In this work, the PC/ABS blend is utilized, which illustrates the improvement of mechanical strength property and several other properties [16]–[18]. Table 3 shows the mixing ratio of PC/ABS. The blended material properties are given in Table 4.

TABLE 3. Mixing ratio of PC/ABS polymers.

Ingredients	Quantity
Acrylonitrile butadiene styrene (ABS)	40 %
Polycarbonate (PC)	60 %

TABLE 4. Properties of blended PC and ABS.

Properties	Parameters	Values
Mechanical	Flexural Strength (psi)	9,800
	Tensile Strength (psi)	5,900
Physical	Density (g/cm³)	1.098
Thermal	Glass Transition Temperature (°C)	125
	Heat Deflection Temperature (°C)	115

B. ENERGY DIRECTOR DESIGN

The EDs design imprinted on the die specimens is used in the injection molding process. EDs design has different shapes like triangular, rectangular, and semi-circular. In this work, the triangular-shaped ED has been selected because it gives a better melting ratio as compared to other EDs. The ED design basically depends on the part of geometry, material, and shape of sonotrode etc. During welding, ED is the primary part to receive maximum ultrasonic energy and starts to melt quickly [7].

C. INJECTION MOLDING

The injection molding process involves several stages like plasticity, melting, homogenizing, and injection. Each stage plays a major role in producing the final mould samples. The concise working of injection molding is explained below. Raw materials of PC/ABS are mixed and fed into the injection molding machine. The machine has heating modules and reciprocating screw. The heating module helps to heat the material and reciprocating screws that are used to convert polymer into a molten state as screws start to rotate continuously. Then the molten polymer is fed into die (cavity) via nozzle at the desired time period. The prepared die setup is shown in Fig. 1. The die temperature is set up below the melting point to bring out the final product in the desired shape. High pressure is applied to reduce the thermal condensation during cooling time.

D. ULTRASONIC POLYMER WELDING PROCESS

The Dukanei Q Series i220 ultrasonic welding equipment with an operating frequency around 20 kHz and power level vary from 1200 to 2400 W [23]. Predefined Dukanei Q Series i220 fixture and sonotrode equipment are used. Q series i220 machine has superior features such as process limits, energy, and distance controllable provisions. The parts should hold tightly, which are to be welded at high pressure and then exposed to constant ultrasonic frequency vibrations of 20 kHz with low amplitude (100–150 μm). The ultrasonic vibration induces stress at the junction of the weld and also this process generates friction at the molecular level leading

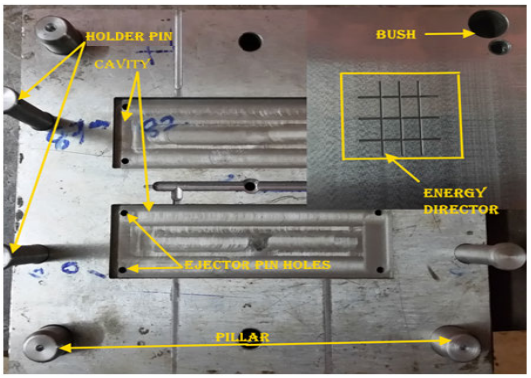

FIGURE 1. Mould setup with imprinted energy directors.

to the melting of the parts [24]. Heat development in ultrasonic welding is considered as an important parameter in thermoplastics. The melting of polymer mainly depends on the selection of processing parameters [20-21] and Energy Directors. The lap joint design is integrated with the energy director as shown in Fig. 2.

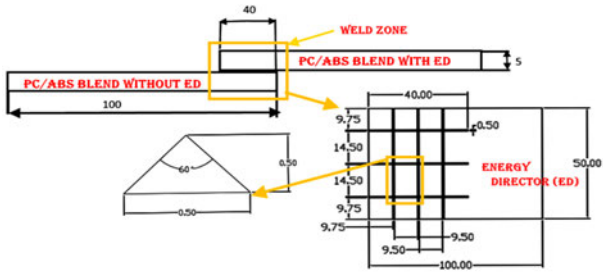

FIGURE 2. Lap joint design incorporated with energy director.

Amorphous and semi-crystalline materials have different properties and melting temperature so that the weld parameters should be chosen based on the material characteristics. The process parameters and corresponding weld strength are presented in Table 5. The strength of weld is measured with the help of Tensile strength measuring instrument (Hydraulic universal testing machine). The machine specifications are Max Load Capacity 2000 kN, Testing Force 2% - 100% of max load, Accuracy ±1%, Max Tensile Space 800 mm and Piston speed:100 mm/min. The ultrasonically welded samples are shown in Fig. 3. The levels of parameters are selected based on the DOE (Design of Experiment). Total 26 samples are prepared based on the Taguchi L9 & L16 orthogonal array. Here, L9 variations are minimum as compared with L16 and also computation of thermal analysis is easier in L16. Therefore, both L9 and L16 models are performed in this work.

E. ARTIFICIAL NEURAL NETWORK MODELLING

Artificial Neural Networks are more noticeable and predominantly utilized for the highly interactive and complex process involved in various real-time applications. The primary reason for implementing the neural network is that it can be

TABLE 5. Process parameter and weld strength.

Sl. No	Pressure (bar)	Weld time (ms)	Amplitude (µm)	Strength (N)
1	3.5	450	100	770.29
2	3.5	450	100	791.68
3	3.5	450	100	803.84
4	3.5	450	110	819.33
5	3.5	500	110	826.58
6	3.5	500	110	798.97
7	4	500	110	798.34
8	4	500	110	785.83
9	4	550	120	792.50
10	4	550	120	813.68
11	4	550	120	858.48
12	4	550	120	833.89
13	4.5	600	120	906.82
14	4.5	600	130	811.84
15	4.5	600	130	807.99
16	4.5	600	130	797.26
17	5	650	130	835.34
18	5	650	130	789.65
19	5	650	140	839.23
20	5	650	140	878.73
21	5	650	140	862.12
22	5.5	700	140	827.76
23	5.5	700	150	815.90
24	6	750	150	847.24
25	6	750	150	840.93
26	6	750	150	826.43

modeled using real-time data without considering any assumptions. There are varieties of ANNs exploited in different modeling techniques such as Radial Basis Function (RBF), MultiLayer Perception (MLP), and Self-Organizing Map (SOM), among others. In this work, a multilayer perception-based ANN model is adopted due to high fault tolerance capacity and generalization and simulation is carried out using MATLAB R2016a. I7 Core Intel Processor with 8 GB RAM has been used for computing. The large number of processing values are taken for modeling the weld strength to predict the accurate value [22]. A data set comprises of 3 - input layers, 1- output layer and 1- hidden layer. The input layer consists of 3- input neurons corresponding to three key parameters such as welding time, pressure and amplitude. The input data accepted via the input layer and hidden layer processing of the ANN is indicated in Eq.1 and Eq.2.

$$a_i^{(1)}(x) = net_i^{(1)} \tag{1}$$

$$b_i^{(1)}(x) = f_i^{(1)}[net_i^{(1)}(x)] = net_i^{(1)}(x), \quad i = 1, 2, 3 \tag{2}$$

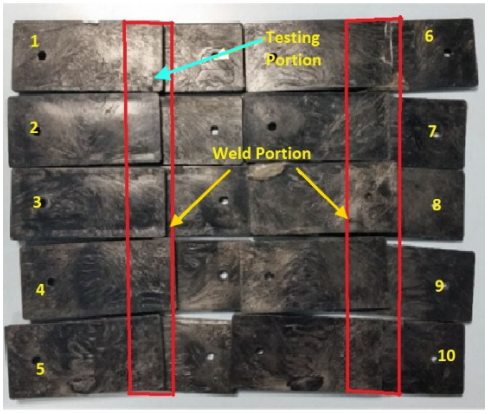

FIGURE 3. Ultrasonically welded PC/ABS blend.

where $a_i^{(1)}$ - input layer with node i,
$net_i^{(1)}$ - sum of input layers and
$b_i^{(1)}$ - hidden layer with node i

The neurons present in the hidden layer are connected to the neurons present in the output layer by using purelin transfer function. Levenberg-Marquardt algorithm is applied for MLP network as a training function. An output neuron with (Nk) node brings out the top optimized weld strength value. The output is the sum of the incoming signals as expressed in Eq.3 and Eq.4.

$$net_k^{(3)} = \sum_j w_j b_j^{(2)}(x) \tag{3}$$

$$N_k^{(3)}(x) = f_k^{(3)} net_k^{(3)}(x)\} = net_k^{(3)}(x) \tag{4}$$

Here, wj represents the weights between the hidden and the output layers.

The best optimized weld strength value has been calculated by modifying and adjusting the weights present in between the layers and learning parameters. In addition to the analysis, the relationship between tensile shear strength and dynamic resistance signal is also estimated. The model for parameter optimization in predicting the relationship between weld strength value and specimen for the proposed network is depicted in Fig. 4.

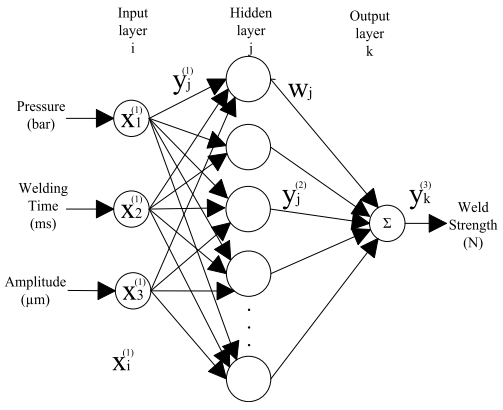

FIGURE 4. Architecture of the proposed ANN-based model.

F. ANFIS MODELLING

Artificial intelligence approach such as fuzzy logic controller and neural network techniques are combined to form a modeling technique known as ANFIS. It has several advantages such as adaption for changing environments inherited from neural networks and pattern recognition. Due to above mentioned advantages, ANFIS is widely preferred in practical case studies especially in studies involving high uncertainty [22].

The set of data chosen for checking and training in the ANFIS regression model is constructed with the help of similar checking and data sets used in regression models. Once initialization is completed, the ANFIS model is trained using MATLAB with the constructed database. In different models, the number of clusters defining the membership function has been estimated to be three experimentally. The input and output variable relationships are obtained from the rule-based mechanism. The rules are defined by extracting knowledge from experience, literature, and statistics. In general, the number of rules is fixed to three from the developed model. A fuzzy proposition or linguistic expression has been assigned for each membership function [22]. From the available types of membership function, Gaussian membership function is chosen because of its concise notation, smoothness and non-zero output at all points. Fig. 5 illustrates the proposed ANN model with 5- layers. In the first layer, each input node consists of an adaptive node and parameter triggering function. The output from this node is used to estimate the membership function that implements the suitable fuzzy value. Each membership function (MF) presents in the network is represented and tuned using different parameters in the learning process. The membership function is represented in Eq.5.

$$\mu_a(x) = \frac{1}{1 + \left|\frac{x - C_i}{A_i}\right|^{2B}} \tag{5}$$

where A_i, B, C_i are the parameter set and $\mu_a(x)$ value lies in the span of 0 to 1. The Normal Distribution (Bell-shaped) function and membership function will be changed according to parameter variation.

In second layer, each node is stable and its output is the product of the input signals. Every node indicates the strength of the rule as denoted in Eq. 6.

$$O_{2,i} = \omega = \mu_a(x).\mu_b(x) \tag{6}$$

where O_2,i corresponds to the output layer 2.

In third layer, the nodes are fixed which compute the ratio of the i^{th} rules strength. Eq.7 represents the output as normalized firing strength.

$$O_{3,i} = (\omega_1 \times \varpi)/(\omega_1 + \omega_2) \tag{7}$$

In fourth layer, all nodes are adaptive nodes. The correlation derived from the input and output layers are given in Eq. 8.

$$O_{4,i} = \varpi_i f_i = \varpi_i (P_i x + Q_i y + R_i) \tag{8}$$

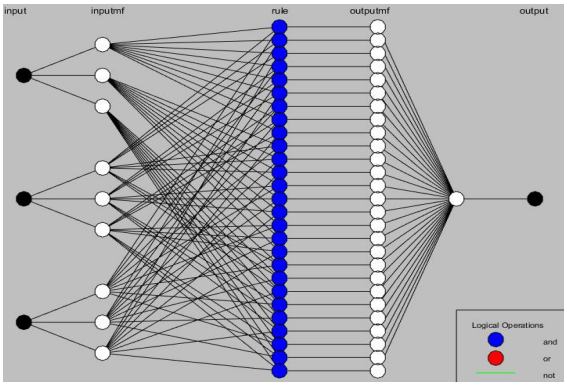

FIGURE 5. Architecture of the proposed ANFIS model.

In fifth layer, the nodes are fixed and output is the sum of all input signals as specified in Eq. 9.

$$O_{5,i} = \sum \varpi_i f_i = \frac{\sum_i \omega_i f_i}{\sum_i \omega_i} \tag{9}$$

The ANFIS identifies the rule automatically and adjusts its membership function parameters accordingly. The goal of this training algorithm is to regulate these parameters to build the ANFIS model and the output should be aligned with the trained data as depicted in Fig. 5.

III. RESULT AND DISCUSSIONS

A. THE INFLUENCE OF INPUT PARAMETER ON THE WELD STRENGTH

The materials weld strength are primarily determined through USW parameters and mode of material preparation. Moreover, the blending combination of two different materials also plays a major role in material weld strength. Many parameters get varied during the welding process, but not all of these parameters influence the weld strength directly. The Pressure is the most influencing parameter that affects the joint strength. If the pressure is low, the static force applied to the material via horn will lessen the force ensuring reduced melt flow. This insufficient melting will reduce the material bonding and in turn affect the weld strength. As the weld strength becomes low, the material bonding also gets reduced. Thus, voids and cavity are created between joints resulting in joint failure. Fig.6 (a) shows the influence of pressure on the weld strength with different pressure values.

The weld time also influences the weld strength. Due to the higher volume of melting, the connection between horn and parts remains for a longer period, hence increasing the weld strength at a particular range. The boding between materials is comparatively low if improper melting in the material happens, thus decreasing the weld strength. Fig. 6 (b) shows welding time over weld strength influencing all parameter values. Hence, it can be concluded that all selected weld time values contribute to the weld strength effectively.

Another major influencing parameter is amplitude and the contribution of individual value to the weld strength; see Fig.6 (c). The heating rate of the material mainly depends on

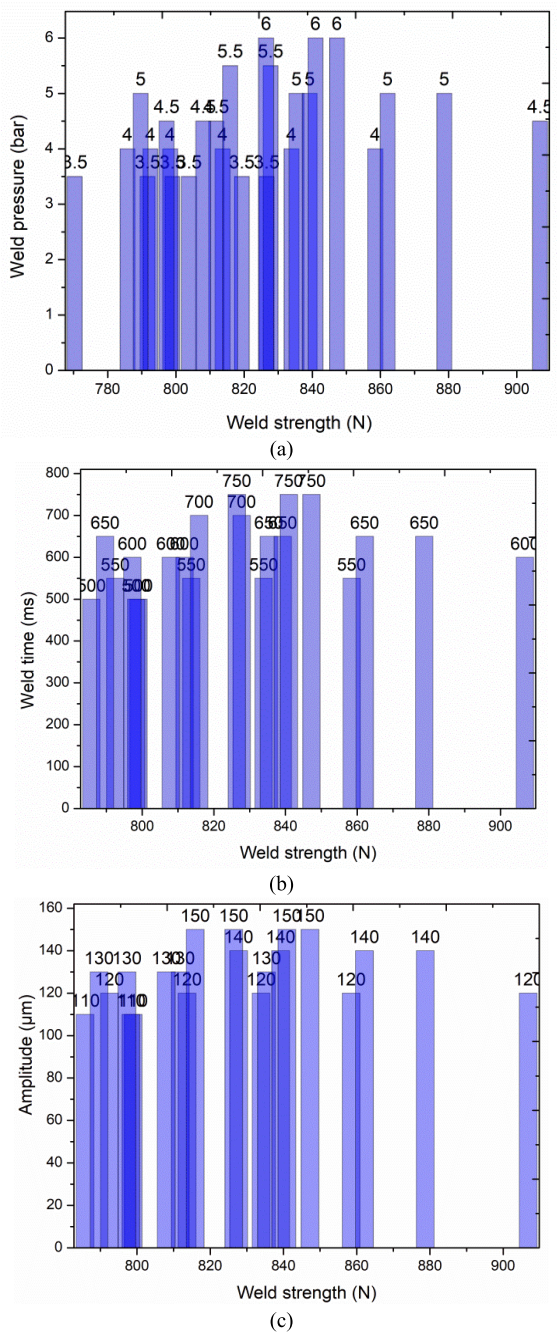

FIGURE 6. (a) Applied pressure Vs weld strength. (b) Weld time vs Weld strength. (c). Amplitude vs Weld strength.

the amplitude applied to the material. The average heating rate (Q_{avg}) is calculated using Eq. (10). Q_{avg} depends on the frequency (ω), complex loss modulus of the material (E''), and the applied strain (ε_o):

$$Q_{avg} = \omega \varepsilon_o^2 E'' / 2 \tag{10}$$

The E'' of the material strongly depends on the temperature. As E'' increases, the conversion of applied amplitude to thermal energy also increases. The temperature increases rapidly when heating is initiated on the energy director. Here, ε_o is directly proportional to the horn amplitude. The heating

produced in the energy director can be streamlined by controlling the amplitude. If the amplitude value is high, then the heating rate of the weld interface will also be high. The rise in temperature will increase the molten material flow, which in turns fastens the molecular alignment. The high amplitude value is necessary to initiate the energy director melting due to semi-crystalline materials.

B. ANN PREDICTION

It is very important to design a model that predicts weld strength with high accuracy. There exist several analysis methods in the various platforms, but ANN is found to be a very effective method to find the weld strength. The relationship between the tensile strength and input process parameters are predicted using multiple layer perceptron-based ANN mode and the simulation is carried out using MATLAB [22]. Here, all the 26 samples are used for training, testing ANN and ANFIS models.

During training process, a set of input training sample (a_i) is taken and forwarded to the input layer of the ANN. The output N_K are obtained from the corresponding input sets consequently. Later, the predicted values are acquired from the neural network model which is compared against the experimentally evaluated weld strength (Y_d). The mean sum of the squared error (MSE) is calculated using Eq. 11.

$$MSE = (Y_d - N_K)^2 \tag{11}$$

where, NK is the predicted value and Yd is the experimental value of weld strength.

From the obtained results, it is deduced that the weld strength can be predicted more accurately using ANN model and best fit line is measured from the regression coefficients as shown in Fig. 7.

It is clear that the performance, testing error, and RMS training error of the model should be based on the number of training data sets available in it. As the number of data sets is limited, it affects the efficiency of the model gradually. The factors like training data, quantity of layers and iteration counts decide the model to prevent from under fit or over fit. Moreover, the neural network model can be predicted easily with least value of RMS testing error. From the experimental and prediction results, it is proven that the designed model gives better performance within the particular limits of training data samples. The comparison of predicted values versus experimentally measured values of weld strength is depicted in Fig. 8. From this comparison graph, the best matching between measured and simulated ANN values are analyzed. However, obtained ANN results matches with most experimental values, but it is not an accurate prediction for all the parameters. Few variations are observed from the ANN results and these variations can change the material melting behavior and influence the phase change (amorphous to semi-crystalline) of the material. The predicted values must be more accurate to find the melting rate of energy director as well as with melt flow direction.

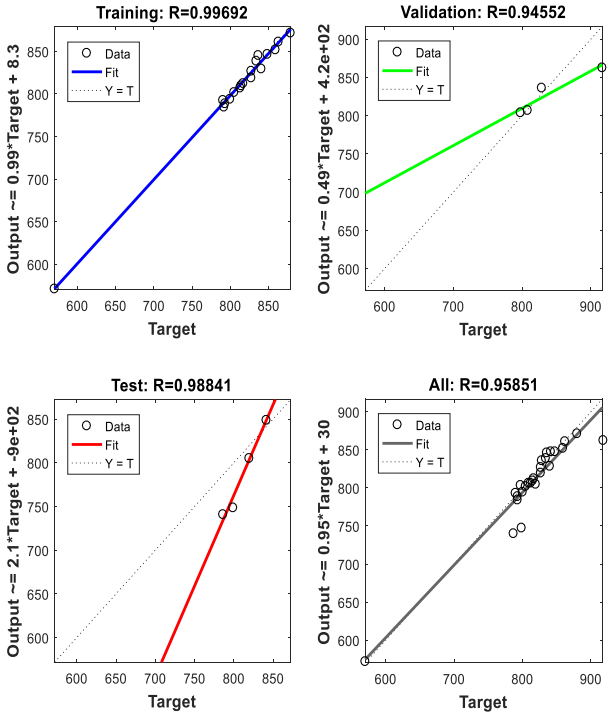

FIGURE 7. Regression analysis.

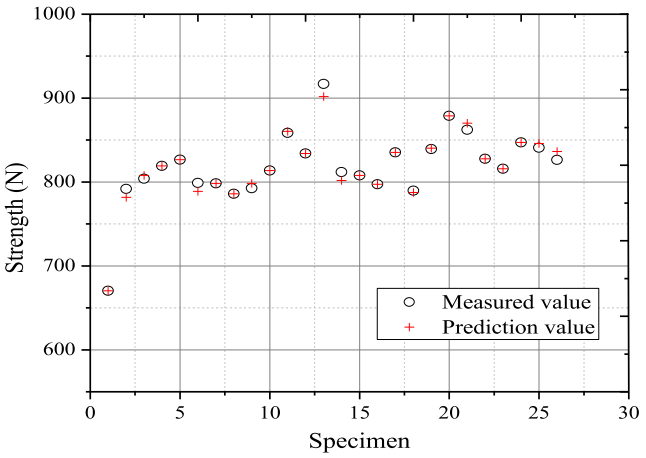

FIGURE 8. Comparison of Weld strength between measured and predicted values.

C. ADAPTIVE NEURO-FUZZY INFERENCE SYSTEM

The ANFIS simulation and experimental results are compared and illustrated in Fig. 9. ANFIS technique presents a precise prediction technique between the simulation and experimentally measured values. Generally, the designed ANFIS model is found to be more sensitive than regression-based models [25]. The minute change occurs any parameters are easily revealed in ANFIS model.

It is clear from the analysis that the designed model is found to be more reliable than the conventional ANN model [26]. In conventional approach, the codes yielded are scattered highly because of difference in sample construction process and experimental setup. Whereas, ANFIS brings out a

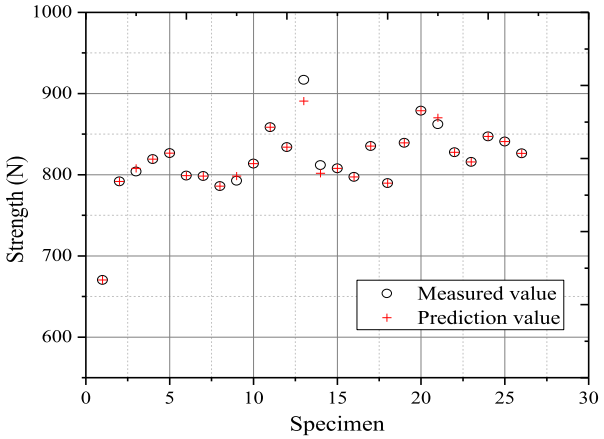

FIGURE 9. Comparison graph between the measured and predicted variables.

better performance [27] than ANN since it yields a better conformance to the current data sets due to high learning capacity (better performance indicators for checking data set). The structure of model is constructed using given data sets and it does not utilize the predefined mathematical equation, which is expressed in terms of input and output variables [28]. The accuracy of ANFIS model prediction depends on data coverage distribution used by database and limited range.

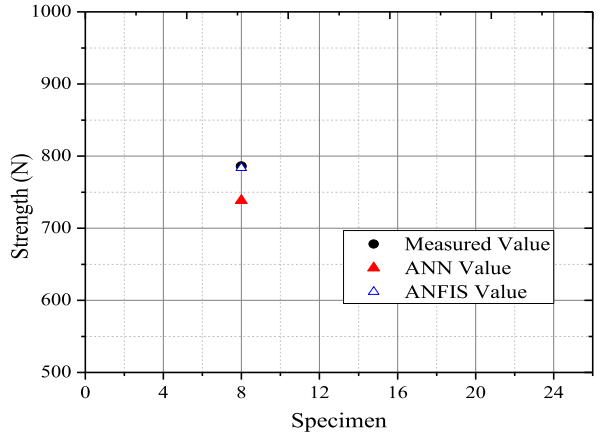

FIGURE 10. Strength comparison for measured value along with ANN and ANFIS.

Furthermore, ANFIS model can be trained and better results are obtained by providing new training samples once a new database becomes available [29], [30]. Fig. 10 shows the comparison of all three (measured, ANN and ANFIS) values for better understanding between the measured and AI techniques. It is proved that the best prediction of tensile strength is obtained by ANFIS prediction. The computation error between ANN and ANFIS is 0.02. (ANN – 0.08 and ANFIS 0.06). The computation time taken for the ANN is approximately 2 mins and ANFIS is approximately 1.8 mins.

D. SCANNING ELECTRON MICROSCOPE ANALYSIS

It is important to analyze the deformed polymer morphology to determine the shape of welded joints [23]. The presence of

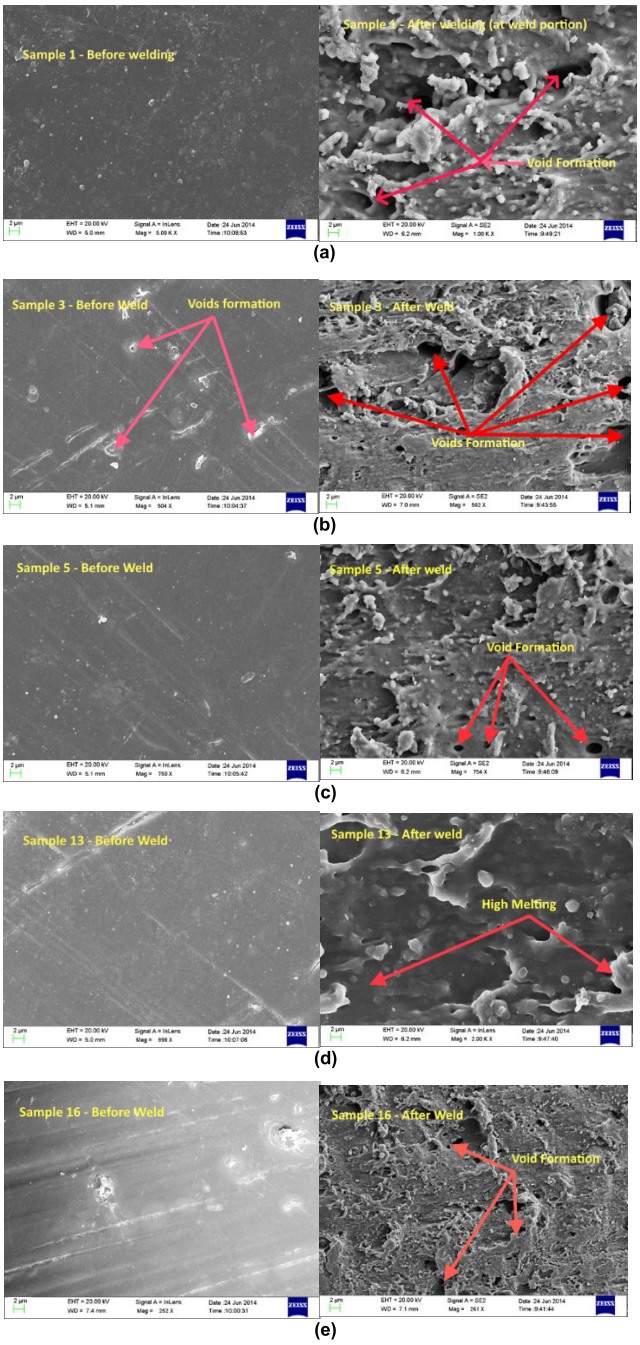

FIGURE 11. SEM analysis: Non-welded and welded region of sample no. 1,3,5,13 &16 (Samples are considered for analysis based on the tensile strength interval of 20 values) (a) Sample 1 (b) Sample 3 c) Sample 5 d) Sample 13 e) Sample 16.

deformed ridges is one of the most important features in the welded sample. The depth and number of deformed ridges indicate temperature, welding time, and weld pressure content. During the short duration of welding time, the intensity of interpenetration remains small. Likewise, the energy and strength also get reduced at the junction of the welding [31]. Fig. 11 demonstrates the images obtained from SEM for a variety of samples with several blend ratios of PC/ABS. The white particles present in the figure are known as peaks.

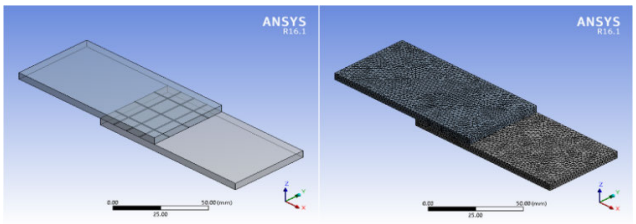

FIGURE 12. Basic model of energy director and mesh.

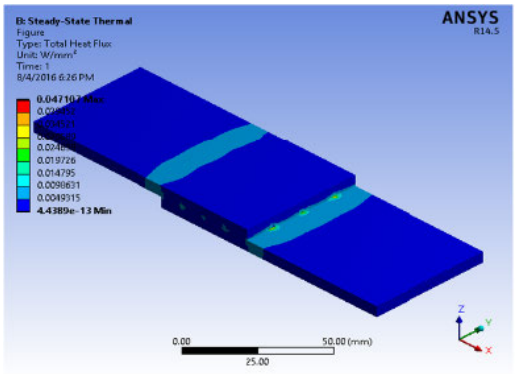

FIGURE 13. Heat initiation at energy director.

A large number of peaks denotes energy directors with good melting points. For SEM analysis, the non-welded and welded region of sample no. 1, 3, 5, 13 & 16 has been taken. Samples are considered for analysis based on the tensile strength interval of 20 values.

E. FINITE ELEMENT ANALYSIS

The finite element modeling (FEM) is used to validate the experimental values. To predict the ultrasonic frequency heat generation during the welding process FEM model is developed. From this model, the changes in temperature distribution, heat flux and strain in polymers can be evaluated. Finite element analysis (FEA) is used after employing the welding process of polymers to understand the heat flex distribution. There are two major platforms such as mechanical and thermal fields are coupled together in an ultrasonic welding process.

Thermal field influences the mechanical field because most of the mechanical properties are sensitive to the temperature. Also, the heat generated from the mechanical field influences the thermal field. When the performance is carried out in FEM analysis, the material property and quantity may be varied based on the simulation run time. If run time is higher, the material property will be reduced and leads to loose the material nature. Fig. 12 to Fig. 16 provide the numerical results of thermal stress data for the welded samples. Fig. 12 shows the initial modeling of energy director and mesh creation in FEM. Fig. 13 shows the initial heat generation due to ultrasonic vibration. Fig. 14 shows the initial melting region (in energy director) and heat flex generation. Fig. 15 gives the total heat flex generation during welding and material melting. Fig. 16 shows the clamping force influence on the material during welding.

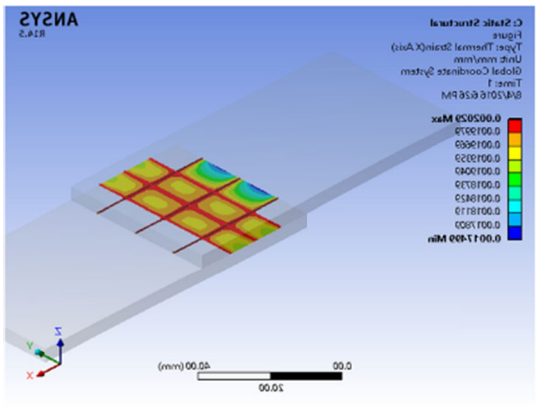

FIGURE 14. Total heat flux generation the starting of the welding at the energy director (initial melting happening at energy director).

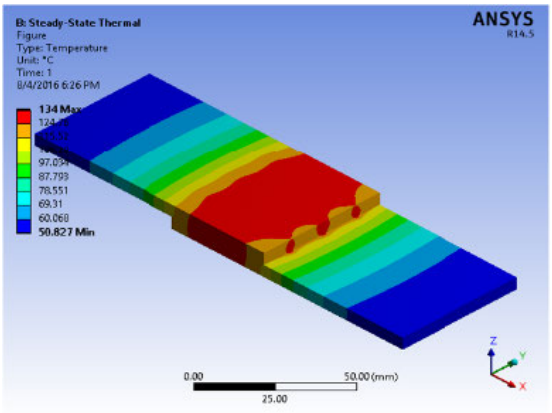

FIGURE 15. Total heat flux generated at energy director side.

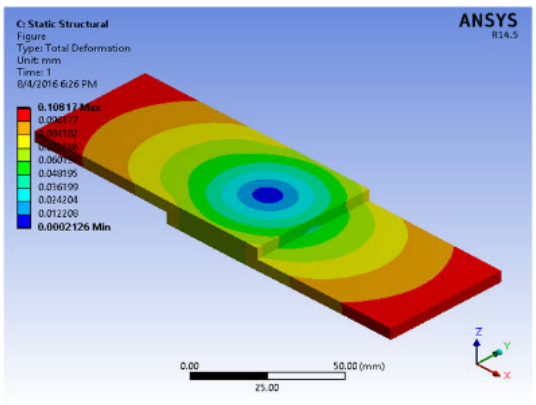

FIGURE 16. Clamping the PC/ABS sample in fixture which generate heat during the welding process.

The plastic strain is relatively small on a certain axis. It is observed that the edge of contact surface at near point of loading has the highest plastic strain. A very few locations particularly at the energy directors, it is observed that the plastic strain in the center of the contact surface exceeds the level of plastic strain at the edge. The value and distribution of plastic deformation reaches the steady state level after a certain number of vibration cycles. Here, the triangular energy

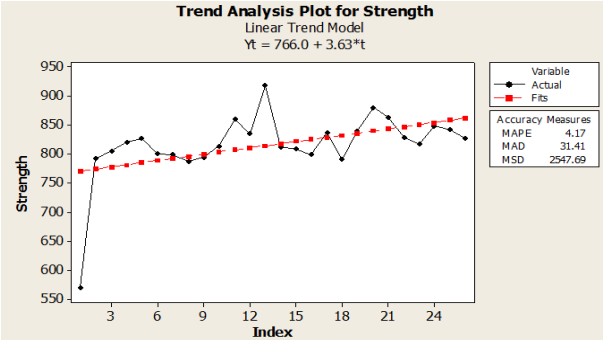

FIGURE 17. Trend analysis of experimental value and predicted value (Minitab).

director experiences the maximum plastic strain which is located at the vertex and the plastic strain distribution has done due to the cyclic vibrations.

F. TREND ANALYSIS FOR WELD STRENGTH

The linear trend model is examined using the Minitab software in order to estimate the strength fit values. Fig. 17 shows the trend analysis of actual (experimental values) versus fit line. From this graph, it is clearly evident that the maximum actual points are fitted with the fit line. The maximum strength for various peak levels is also obtained when the weld pressure and weld time is maximum.

IV. CONCLUSION

PC/ABS material has been joined together using ultrasonic polymer welding with different weld parameter ranges. Total 26 samples are prepared and welded with different input parameters such as weld time, amplitude and pressure. Samples are tested in the tensile machine. From the experimental result, the minimum and maximum values of tensile is 770.29 N to 906.29 N. The tensile value of each sample is analyzed using ANN and ANFIS in order to predict the best input parameter value. Thus, the best prediction has been obtained from the ANFIS with less error. The SEM images have been analysed to identify the direction of molten material during welding and to realize the nature of melting. SEM analysis discloses that the higher vibration causes more melting in the material and also taking longer curing time which will reduce the strength of the weld. Likewise, the weld strength of the material has appeared to be more with higher input amplitude. On the other hand, lesser input amplitude may produce the voids leads to reduce the weld strength of the material. For better understanding the melting and weld strength of the material, the ANSYS heat flow simulation has been performed. From the ANSYS results, it is clearly understood that the melting is started from the energy director and its moving towards to the other parts. So, the even heat distribution has been done in the material which leads to increase the weld strength. Trend analysis is performed in order to find the best fit value. The mid-range value from this analysis is the optimal for the fit value.

REFERENCES

[1] A. Elzwayie, A. El-shafie, Z. M. Yaseen, H. A. Afan, and M. F. Allawi, "RBFNN-based model for heavy metal prediction for different climatic and pollution conditions," *Neural Comput. Appl.*, vol. 28, no. 8, pp. 1991–2003, Aug. 2017.
[2] J.-C. Huang and M.-S. Wang, "Recent advances in ABS/PC blends," *Adv. Polym. Technol.*, vol. 9, no. 4, pp. 293–299, 1989.
[3] R. Krache and I. Debah, "Some mechanical and thermal properties of PC/ABS blends," *Mater. Sci. Appl.*, vol. 2, no. 5, pp. 404–410, 2011.
[4] S. Shimada, H. Tanaka, K. Hasebe, N. Hayashi, Y. Ochi, T. Matsui, I. Nishizaki, Y. Matsumoto, Y. Tanaka, H. Nakamura, Y. Mizuno, and K. Nakamura, "Ultrasonic welding of polymer optical fibres onto composite materials," *Electron. Lett.*, vol. 52, no. 17, pp. 1472–1474, Aug. 2016.
[5] H.-S. Shin, M. A. Diaz, Z. M. Bautista, and S. Awaji, "Joint resistance characteristics in ultrasonic weld REBCO CC tapes at various temperatures and magnetic fields," *IEEE Trans. Appl. Supercond.*, vol. 28, no. 4, pp. 1–5, Jun. 2018.
[6] D. Grewel, *Plastics and Composites Welding Handbook*. New York, NY, USA: Hanser, 2013.
[7] X. Li, C. Lu, L. Gao, S. Xiao, and L. Wen, "An effective multiobjective algorithm for energy-efficient scheduling in a real-life welding shop," *IEEE Trans. Ind. Informat.*, vol. 14, no. 12, pp. 5400–5409, Dec. 2018.
[8] C. K. Das, A. Malas, P. Pal, S. Friedrich, and M. Gehde, "Ultrasonic welding of amorphous and semi crystalline materials," *Adv. Mater. Res.*, vol. 716, pp. 271–275, Jul. 2013.
[9] H. Lais, P. S. Lowe, L. C. Wrobel, and T.-H. Gan, "Investigation of ultrasonic sonotrode design to improve the performance of ultrasonic fouling removal," *IEEE Access*, vol. 7, pp. 148897–148912, 2019.
[10] M. F. A. Zaharuddin, D. Kim, and S. Rhee, "An ANFIS based approach for predicting the weld strength of resistance spot welding in artificial intelligence development," *J. Mech. Sci. Technol.*, vol. 31, no. 11, pp. 5467–5476, Nov. 2017.
[11] Y. Yan, D. Liu, B. Gao, G. Y. Tian, and Z. C. Cai, "A deep learning-based ultrasonic pattern recognition method for inspecting girth weld cracking of gas pipeline," *IEEE Sensors J.*, vol. 20, no. 14, pp. 7997–8006, Jul. 2020.
[12] E. Boldsaikhan, E. M. Corwin, A. M. Logar, and W. J. Arbegast, "The use of neural network and discrete Fourier transform for real-time evaluation of friction stir welding," *Appl. Soft Comput.*, vol. 11, no. 8, pp. 4839–4846, Dec. 2011.
[13] N. D. Ghetiya and K. M. Patel, "Prediction of tensile strength in friction stir welded aluminium alloy using artificial neural network," *Procedia Technol.*, vol. 14, pp. 274–281, 2014.
[14] E. Rezaei, A. Karami, T. Yousefi, and S. Mahmoudinezhad, "Modeling the free convection heat transfer in a partitioned cavity using ANFIS," *Int. Commun. Heat Mass Transf.*, vol. 39, no. 3, pp. 470–475, Mar. 2012.
[15] M. Hayati, A. M. Rashidi, and A. Rezaei, "Prediction of grain size of nanocrystalline nickel coatings using adaptive neuro-fuzzy inference system," *Solid State Sci.*, vol. 13, no. 1, pp. 163–167, Jan. 2011.
[16] J. J. Herpels and L. Mascia, "Effects of styrene-acrylonitrile/butadiene ratio on the toughness of polycarbonate/ABS blends," *Eur. Polym. J.*, vol. 26, no. 9, pp. 997–1003, Jan. 1990.
[17] M. H. Yazdi and P. Lee-Sullivan, "Determination of dual glass transition temperatures of a PC/ABS blend using two TMA modes," *J. Thermal Anal. Calorimetry*, vol. 96, no. 1, pp. 7–14, Apr. 2009.
[18] D. Quintens, G. Groeninckx, M. Guest, and L. Aerts, "Mechanical behavior related to the phase morphology of PC/SAN polymer blends," *Polym. Eng. Sci.*, vol. 30, no. 22, pp. 1474–1483, Nov. 1990.
[19] B. B. Difallah, M. Kharrat, M. Dammak, and G. Monteil, "Mechanical and tribological response of ABS polymer matrix filled with graphite powder," *Mater. Des.*, vol. 34, pp. 782–787, Feb. 2012.
[20] K. Pielichowski, A. Leszczyska, and J. Njuguna, "Mechanisms of thermal stability enhancement in polymer nanocomposites," in *Optimization of Polymer Nanocomposite Properties*. Hoboken, NJ, USA: Wiley, 2010, pp. 195–210.
[21] L.-D. Zhao, S.-H. Lo, Y. Zhang, H. Sun, G. Tan, C. Uher, C. Wolverton, V. P. Dravid, and M. G. Kanatzidis, "Ultralow thermal conductivity and high thermoelectric figure of merit in SnSe crystals," *Nature*, vol. 508, no. 7496, pp. 373–377, Apr. 2014.
[22] A. N. Ahmed, C. W. M. Noor, M. F. Allawi, and A. El-Shafie, "RBF-NN-based model for prediction of weld bead geometry in shielded metal arc welding (SMAW)," *Neural Comput. Appl.*, vol. 29, no. 3, pp. 889–899, Feb. 2018.

[23] F. Köhler, I. F. Villegas, C. Dransfeld, and A. Herrmann, "Static ultrasonic welding of carbon fibre unidirectional thermoplastic materials and the influence of heat generation and heat transfer," *J. Compos. Mater.*, 2021, doi: 10.1177/0021998320976818.
[24] G. Zhang, J. Qiu, E. Sakai, and Z. Zhou, "Interface investigation between dissimilar materials by ultrasonic thermal welding by the third phase," *Int. J. Adhes. Adhesives*, vol. 104, Jan. 2021, Art. no. 102722.
[25] A. Abraham, "Adaptation of fuzzy inference system using neural learning," in *Fuzzy Systems Engineering Studies in Fuzziness and Soft Computing*. Berlin, Germany: Springer, 2005, pp. 53–83.
[26] A. Fathi and A. Mozaffari, "Vector optimization of laser solid freeform fabrication system using a hierarchical mutable smart bee-fuzzy inference system and hybrid NSGA-II/self-organizing map," *J. Intell. Manuf.*, vol. 25, no. 4, pp. 775–795, Aug. 2014.
[27] M. W. Dewan, D. J. Huggett, T. Warren Liao, M. A. Wahab, and A. M. Okeil, "Prediction of tensile strength of friction stir weld joints with adaptive neuro-fuzzy inference system (ANFIS) and neural network," *Mater. Design*, vol. 92, pp. 288–299, Feb. 2016.
[28] R. Sudhakaran, V. Vel Murugan, P. S. Sivasakthivel, and M. Balaji, "Prediction and optimization of depth of penetration for stainless steel gas tungsten arc welded plates using artificial neural networks and simulated annealing algorithm," *Neural Comput. Appl.*, vol. 22, nos. 3–4, pp. 637–649, Mar. 2013.
[29] R. Tuntas and B. Dikici, "An ANFIS model to prediction of corrosion resistance of coated implant materials," *Neural Comput. Appl.*, vol. 28, no. 11, pp. 3617–3627, Nov. 2017.
[30] J. Wróbel and A. Kulawik, "Calculations of the heat source parameters on the basis of temperature fields with the use of ANN," *Neural Comput. Appl.*, vol. 31, no. 11, pp. 7583–7593, Nov. 2019.
[31] J. Sun, C. Li, X.-J. Wu, V. Palade, and W. Fang, "An effective method of weld defect detection and classification based on machine vision," *IEEE Trans. Ind. Informat.*, vol. 15, no. 12, pp. 6322–6333, Dec. 2019.

T. CHINNADURAI received the B.E. degree in electronics and instrumentation engineering from Anna University, Chennai, in 2012, the M.E. degree in mechatronics engineering from Anna University, Chennai, in 2014, and the Ph.D. degree from the School of Electrical Engineering (SELECT), Vellore Institute of Technology (VIT), Vellore, in 2017. He is currently working as an Associate Professor with the Department of Instrumentation and Control Engineering, Sri Krishna College of Technology, Coimbatore. His research interests include battery management, polymers, welding, and thermal analysis.

NATARAJAN PRABAHARAN (Member, IEEE) received the B.E. degree in electrical and electronics engineering and the M.E. degree in power electronics and drives from the affiliated college of Anna University, Chennai, India, in 2012 and 2014, respectively, and the Ph.D. degree in energy and power electronics from the Vellore Institute of Technology (VIT) University, Vellore, India, in 2017. He is currently an Assistant Professor with the Department of Electrical and Electronics Engineering, SASTRA Deemed University, Thanjavur, India. His research interests include power electronics, new topologies for inverter and converters, grid integration of renewable energy sources and their controllers, photovoltaic systems, and microgrid. He is a technical program committee member for many reputed international conferences. He was a recipient of two prestigious travel grants under the category of Young Scientist from the Science and Engineering Research Board and Asian Development Bank, in 2015 and 2016, respectively. He was a recipient of the University Merit Ranker Award in 2014. He serves as an Associate Editor for the *IET Renewable Power Generation*, *International Transactions on Electrical Energy Systems*, IEEE Access, *Journal of Power Electronics*, and *International Journal of Renewable Energy Research*.

S. SARAVANAN received the B.E. degree in electrical and electronics engineering from the Karpagam College of Engineering, Coimbatore, India, in 2012, the M.E. degree in power electronics and drives from the Sri Krishna College of Engineering and Technology, Coimbatore, India, in 2014, and the Ph.D. degree from VIT University, Vellore, India, in 2017. He is currently an Assistant Professor with the Department of Electrical and Electronics Engineering, Sri Krishna College of Technology, Coimbatore. His areas of interests include power electronics and applications of power electronics in renewable energy systems.

M. KARTHIGAI PANDEAN was born in Madurai, India, in 1981. He received the B.Eng. degree from the Department of Electronics and Instrumentation, Karunya Institute of Technology, Coimbatore, the master's degree in applied electronics from Anna University, Chennai, in 2002 and 2006, respectively, and the Ph.D. degree in the area of semiconductor device modelling from Thiagarajar College of Engineering, Madurai, in 2015. He has 15 years of experience as an academician and is currently employed as an Associate Professor with the Department of Instrumentation and Control Engineering, Sri Krishna College of Technology, Coimbatore. His research interests include VLSI device modelling, nanoelectronics and the design of antenna.

P. PANDIYAN was born in Aruppukottai, Tamil Nadu, India, in 1985. He received the bachelor's degree in electrical and electronics engineering from Anna University, Chennai, India, in 2006, the master's degree from the Department of Electronics and Communication Engineering, Sathyabama University, Chennai, India, in 2010, and the Ph.D. degree in instrumentation and control engineering from the National Institute of Technology, Tiruchirappalli, India, in 2018. He is currently working as an Assistant Professor with the Electrical and Electronics Engineering Department, Sri Krishna College of Technology, Coimbatore. His research interests include the design and simulation of MEMS-based logic devices and energy harvesting.

HASSAN HAES ALHELOU (Senior Member) is currently a Faculty Member at Tisheen University, Lattakia, Syria. He has published more than 100 research papers in high-quality peer-reviewed journals and international conferences. He has also performed more than 600 reviews for high prestigious journals, including the IEEE Transactions on Industrial Informatics, IEEE Transactions on Industrial Electronics, *Energy Conversion and Management*, *Applied Energy*, and *International Journal of Electrical Power & Energy Systems*. He has participated in more than 15 industrial projects. His major research interests are power systems, power system dynamics, power system operation and control, dynamic state estimation, frequency control, smart grids, microgrids, demand response, load shedding, and power system protection. He is included in the 2018 and 2019 Publons list of the top 1% best reviewer and researchers in the field of engineering. He was a recipient of the Outstanding Reviewer Award from the *Energy Conversion and Management Journal* in 2016, *ISA Transactions Journal* in 2018, *Applied Energy Journal* in 2019, and many other awards. He was a recipient of the best young researcher in the Arab Student Forum Creative among 61 researchers from 16 countries at Alexandria University, Egypt, in 2011.